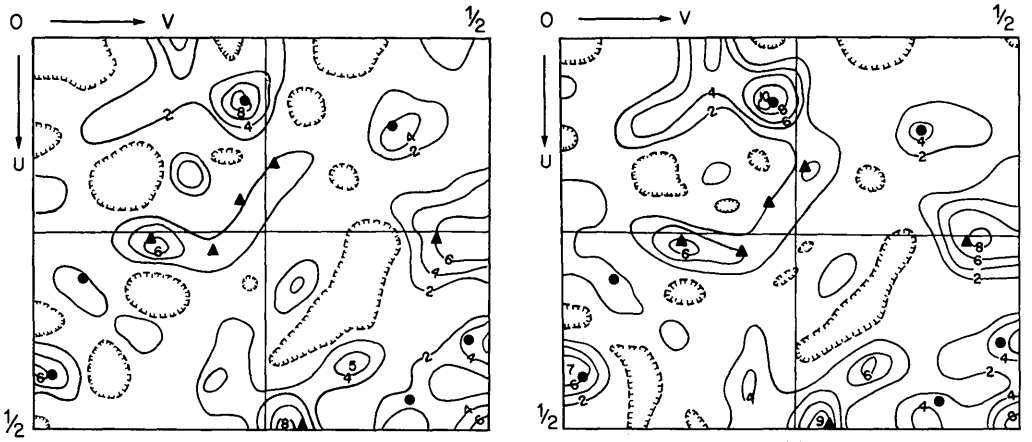

Fig. 4. Projections *UV* 1/2 of the difference Patterson synthesis of the $Hg(SCH_2CH_2NH_3Cl)_2$ derivative of γ-crystallin IIIb. Overall scale and temperature coefficients are calculated (*a*) using the relation $\sum (F_p^N)^2/\sum (F_{pH}^D)^2$ and (*b*) using formula (13) of this paper.

be added that the use of this principle changes significantly only the scale factors of the strong derivatives. For the weak derivatives these changes are small. Finally, it may be noted that the use of the direct method of calculation of scale factors does not require essential changes in the computer program.

I am indebted to Dr Yu. N. Chirgadze for constant interest and help throughout this work.

References

ARNONE, A., BIER, C. J., COTTON, F. A., DAY, V. W., HAZEN, E. E. JR, RICHARDSON, D. C., RICHARDSON, J. S. & YONATH, A. (1971). *J. Biol. Chem.* **246**, 2302–2316.

BLOW, D. M. (1958). *Proc. R. Soc. London Ser. A*, **247**, 302–335.

BLUNDELL, T. L. & JOHNSON, L. N. (1976). *Protein Crystallography*, pp. 333–336. New York, London, San Francisco: Academic Press.

CHIRGADZE, YU. N., SERGEEV, YU. V., FOMENKOVA, N. P. & ORESHIN, V. D. (1981). *FEBS Lett.* **131**, 81–84.

CRICK, F. H. C. & MAGDOFF, B. S. (1956). *Acta Cryst.* **9**, 901–908.

EKLUND, H., SAMAMA, J.-P., WALLEN, L. & BRANDEN, C.-I. (1981). *J. Mol. Biol.* **146**, 561–587.

GREEN, D. W., INGRAM, V. M. & PERUTZ, M. F. (1954). *Proc. R. Soc. London Ser. A*, **225**, 287–307.

HAMILTON, W. C., ROLLETT, I. S. & SPARKS, R. A. (1965). *Acta Cryst.* **18**, 129–130.

KRAUT, J., SIEKER, L. C., HIGH, D. F. & FREER, S. T. (1962). *Proc. Natl Acad. Sci. USA*, **48**, 1417–1430.

SINGH, A. K. & RAMASESHAN, S. (1966). *Acta Cryst.* **21**, 279–280.

TEN EYCK, L. F. & ARNONE, A. (1976). *J. Mol. Biol.* **100**, 3–11.

WILSON, A. J. C. (1949). *Acta Cryst.* **2**, 318–321.

Acta Cryst. (1983). A**39**, 697–706

The Contrast of Defects in Inelastically Scattered Electrons

BY PETER REZ*

Department of Materials Science, University of California, Berkeley, California 94720, *USA*

(*Received* 25 *June* 1979; *accepted* 6 *April* 1983)

Abstract

The theory for the contrast of stacking faults and dislocations in electrons which have been scattered inelastically is derived. Small-angle plasmon and single-electron scattering show similar contrast to the elastically scattered electrons. Phonon scattering by large angles away from strongly excited Bragg reflections shows reversed contrast and small-angle phonon scattering gives better contrast for defects near the top of the specimen.

* Present address: V. G. Microscopes Ltd, Charlwoods Road, East Grinstead, Sussex RH19 2JQ, England.

0108-7673/83/050697-10$01.50

Introduction

In the electron microscopy of crystals greater than about 1000 Å thick, many of the electrons have been inelastically scattered by plasmons, single electrons and phonons.

The loss of electrons from the elastically scattered Bragg beams (due to inelastic scattering) has been considered as an absorption which can be represented by a non-Hermitian addition to the crystal potential (Yoshioka, 1957). There has not been much work on the positive contribution, if any, of inelastically scattered electrons to any image. Howie (1963) argued qualitatively that images observed in plasmon-scattered electrons should be similar to images in elastically scattered electrons. Humphreys & Whelan (1969) and Cundy, Howie & Valdre (1969) argued that the same effects should be true for small-angle single-electron scattering.

There have been some observations that showed contrast preservation for plasmon scattering in perfect crystals (Castaing, El Hili & Henry, 1966) and stacking-fault contrast in single-electron excitations has been observed by Craven, Gibson, Howie & Spalding (1978). Stacking-fault contrast in plasmon-scattered electrons was investigated by El Hili (1967).

The contrast for large-angle scattering by phonons, as first observed by Kamiya & Uyeda (1961), could not be predicted by using simple arguments, and experimentally was shown to be quite weak for stacking faults (Kamiya & Nakai, 1971). Nonoyama, Nakai & Kamiya (1973) also showed a top/bottom effect in the images of stacking faults. Kamiya & Nakai (1976) and Gai & Howie (1975) also investigated the phonon contribution to dislocation images.

Calculations of contrast of dislocations in phonon-scattered electrons (Melander & Sandstrom, 1975*a*) and stacking faults in phonon-scattered and plasmon-scattered electrons (Melander & Sandstrom, 1975*b*; Melander, 1975) have been performed by summing over the 'resonance errors' mentioned by Howie (1963).

In this paper, the theory of Young & Rez (1975) and Rez, Humphreys & Whelan (1977) will be applied to imperfect crystals. This leads to a more compact expression of the theory than that given by Melander & Sandstrom and the expression for stacking-fault contrast can be given in closed form. Furthermore, the theory can be more easily used to give qualitative indications of the contrast to be expected from inelastic excitations.

Theory

Both the incident and inelastically scattered states can be expressed either as sums of plane waves

$$\varphi_n(\mathbf{r}) = \sum_g \varphi_g(z) \exp\,[i(\mathbf{k} + \mathbf{g}).\mathbf{r}] \tag{1}$$

or sums of Bloch waves of energy E_n

$$\varphi_n(\mathbf{r}) = \sum_j \psi^j(z) \sum_g C_g^j \exp\,[i(\mathbf{k}^j + \mathbf{g}).\mathbf{r}] \tag{2}$$

the z direction being normal to the foil surface. The wave functions are solutions of Yoshioka's (1957) equation:

$$\left[\frac{-\hbar^2}{2m}\nabla^2 + H_{nm} - E_n\right] = -\sum_{m\neq n} H_{nm}\,\varphi_m, \tag{3}$$

where the matrix elements $H_{nm}(\mathbf{r})$ are given by

$$H_{nm}(\mathbf{r}) = \int a_n^*(\mathbf{r}_1,\ldots,\mathbf{r}_M) H(\mathbf{r},\mathbf{r}_1,\ldots,\mathbf{r}_M) \times a_M(\mathbf{r}_1,\ldots,\mathbf{r}_M)\,\mathrm{d}\mathbf{r}_1,\ldots,\mathrm{d}\mathbf{r}_M, \tag{4}$$

where a_n is the wave function of the crystal in its nth excited state and H describes the interaction between the fast electron and the crystal. Howie (1963) and Humphreys & Whelan (1969) showed that

$$H_{nm}(\mathbf{r}) = \exp\,(-i\mathbf{q}_{nm}\,\mathbf{r}) \sum_g H_g^{nm}(\mathbf{r}) \exp\,(i\mathbf{g}.\mathbf{r}), \tag{5}$$

where $\mathbf{q}_{nm}$ is the wave vector of the excitation created in the transition $m \to \bar{n}$. The form of $H_{nm}(\mathbf{r})$ for various excitations is discussed in the next section. For single inelastic scattering the amplitudes of the inelastically scattered Bloch waves (denoted throughout this paper by primed indices) and incident electron Bloch-wave amplitudes are related by the differential equation:

$$\frac{\mathrm{d}\psi^{i'}(z)}{\mathrm{d}z} = \sum_j S^{i'j} \exp\,(i\delta k^{i'j}\,z)\,\psi^j(z) \tag{6}$$

$$\delta k^{i'j} = -(k^{i'} - k^j + q)_z, \tag{7}$$

where $k^{i'}$ is the wave vector of the ith scattered Bloch wave, k^j is the wave vector of the jth incident Bloch wave and q is the excitation wave vector defined to lie in the first Brillouin zone. The change in the z component of the fast electron wave vector need not equal the z component of the crystal excitation wave vector given by periodic boundary conditions. $S^{i'j}$ is a matrix element for transitions between branch j of the incident-state dispersion surface and branch i' of the scattered-state dispersion surface and is given by

$$S^{i'j} = \frac{-im}{\hbar^2\,k_z^{i'}} \sum_{lh} C_l^{i'}\,H_{l-h}\,C_h^j, \tag{8}$$

where $k_z^{i'}$ is the z component of k and $C_l^{i'}$ and C_h^j are Bloch-wave coefficients (real for centrosymmetric crystals).

It is helpful for the development of the theory to rewrite (6) in matrix form:

$$\frac{\mathrm{d}\boldsymbol{\psi}'(z)}{\mathrm{d}z} = \mathsf{S}\,(z) \exp\,(-iq_z\,z)\,\boldsymbol{\psi}(0), \tag{9a}$$

where

$$S(z) = S^{i'j} \exp[i(k^j - k^{i'})\, z]. \quad (9b)$$

In a crystal with a stacking fault, the inelastic scattering can take place either before or after the stacking fault. A fault at depth t introduces a phase shift of $\mathbf{g}.\mathbf{R}$ ($\mathbf{R}$ the fault displacement vector) on the plane waves in (1). The change in the Bloch-wave amplitudes can be represented by the matrix operator

$$\psi(t + \delta) = A(t)\, \psi(t - \delta), \quad (10a)$$

where δ is a small change in depth,

$$A(t) = \sum_g C_g^i C_g^j \exp(i\mathbf{g}.\mathbf{R}) \exp[i(k^j - k^i)\, t]. \quad (10b)$$

The amplitude from inelastic scattering after the stacking fault is represented by

$$\int_t^T S(z) \exp(-iq_z z)\, A(t)\, \psi(0)\, dz, \quad (11)$$

and the amplitude from inelastic scattering before the fault is represented by

$$A(t) \int_0^t S(z) \exp(-iq_z z)\, \psi(0)\, dz. \quad (12)$$

The intensity after scattering by a given inelastic excitation is

$$I_g^q = \frac{V}{4\pi^2} d\sigma \sum_{q_z} \left| C'(T) \int_t^T S(z) \times \exp(-iq_z z)\, A(t)\, \psi(0)\, dz + C'(T)\, A(T) \times \int_0^t S(z) \exp(-iq_z z)\, \psi(0)\, dz \right|^2. \quad (13)$$

T being the specimen thickness and $(V/4\pi^2)\, d\sigma$ being the density of inelastic excitation states (V is the crystal volume). It is necessary to sum over all z components of the excitation wave vector for a given wave-vector component in the plane parallel to the specimen surface. The z components of the wave vector are given by periodic boundary conditions

$$q_z = 2\pi n/t.$$

If the matrix elements vary slowly with q_z (which is nearly always the case as q_x is much greater than q_z) the sum can be performed analytically (Young & Rez, 1975; Rez *et al.*, 1977) to give the relation that each slice scatters independently

$$\sum_n \exp\left[i \frac{2\pi n}{t} (z - z')\right] = N_z\, \delta(z - z'), \quad (14)$$

where z, z' refer to lattice sites and N_z is the number of lattice sites in the z direction.

It must be remembered that the crystal modes are only truly independent in a perfect crystal and (13) should contain terms corresponding to correlation between different modes.* This represents the scattering of the crystal excitation by the defect which is in itself a problem of great complexity. Furthermore, it is probably a second-order effect and, for the purposes of fast-electron scattering, it will be assumed that the modes for the imperfect crystal are the same as those of the perfect crystal and that these correlation efforts will be neglected. When the effects of the crystal structure in the z direction are also neglected (for elastic scattering this is the assumption of no upper-layer lines), the sum over lattice sites can be written as an integral. Performing the integration gives

$$I_g^q = \frac{V}{4\pi^2} d\sigma \sum_{k'l'} \sum_{ij} \sum_{i'j'} \sum_{hh'} C_g^{k'} C_g^{l'} C_h^k \times C_{h'}^{l'} C_h^{i'} C_{h'}^{j'} S^{i'j} S^{j'i} C_0^i C_0^j \times \exp[i(k^{k'} - k^{l'})(T - t)] \exp[i(h - h')\, R] \times \frac{\{\exp[i(k^j - k^i)\, t] - \exp[i(k^{i'} - k^{j'})\, t]\}}{i(k^j - k^{i'} - k^i + k^{j'})}$$

$$+ \sum_{i'j'} \sum_{ij} \sum_{kl} \sum_{hh'} C_g^{i'} C_g^{j'} \times S^{i'j} S^{j'i} C_h^j C_{h'}^i C_h^l C_{h'}^k C_0^l C_o^k \times \exp[i(k^l - k^k)t] \exp[i(h - h')R] \times \{\exp[i(k^j - k^l)(T - t)] - \exp[i(k^{i'} - k^{j'})(T - t)]\} \times [i(k^j - k^{i'} - k^l + k^{j'})]^{-1}. \quad (15)$$

The theory for inelastic scattering in a crystal with dislocations proceeds in a similar way. The amplitudes in the presence of a strain field denoted by $\mathbf{u}(\mathbf{r})$ are given by the solution of the coupled differential equation

$$\frac{d\psi^j(z)}{dz} = \sum_g C_g^i C_g^j \mathbf{g} \frac{d\mathbf{u}(\mathbf{r})}{dz} \exp[i(k^j - k^i)\, z]\, \psi^j(z). \quad (16)$$

The plane-wave amplitudes are solutions of the Howie–Whelan equations:

$$\frac{d\varphi_g(r)}{dz} = \sum_h \frac{i\pi}{\xi_{g-h}} \varphi_h(\mathbf{r}) + i\left[2\pi s_g + \mathbf{g} \frac{d\mathbf{u}(\mathbf{r})}{dz}\right] \varphi_g(\mathbf{r}), \quad (17)$$

where s_g is the excitation error and ξ_g is the extinction distance. The solutions of the differential equation at one depth can be expressed as a matrix operation on the solution at another depth (see Appendix *A*)

$$\psi(t_1) = A(t_1 - t_2)\, \psi(t_2). \quad (18)$$

* I am indebted to Dr A. P. Young for pointing this out.

In a crystal where single inelastic scattering and dislocation scattering takes place, it is possible to have scattering from the dislocation both before and after the inelastic scattering. The amplitude at the exit surface of the crystal can be written as

$$\psi'(T) = \int_0^T \mathsf{A}'(T-z)\,\mathsf{S}(z)\exp(-iq_z z)\,\mathsf{A}(z)\,\psi(0)\,\mathrm{d}z \quad (19)$$

(see Appendix *B*). The intensity in a beam at the exit surface is then

$$I_g^q = \sum_{q_z} |C'(T) \int_0^T \mathsf{A}'(T-z)\,\mathsf{S}(z) \times \exp(-iq_z z)\,\mathsf{A}(z)\,\psi(0)\,\mathrm{d}z|^2. \quad (20)$$

The sum over normal modes can again be performed to give the relation that each slice scatters independently, which means that the intensity is given by

$$I_g^q = \frac{V}{4\pi^2} d\sigma \sum\sum C_g^{i'} C_g^{j'} \exp[i(k^{i'} - k^{j'})\,T] \times \int_0^T A^{i'p'}(T-z) A^{*j'q'}(T-z)\,S^{p'q} S^{q'p} \times \exp[i(\Delta k^{p'q} - \Delta k^{q'p})\,z]\,A^{qj}(z) \times A^{*pi}(z)\,C_0^i\,C_0^j\,\mathrm{d}z, \quad (21)$$

where $\Delta k^{p'q'} = k^q - k^{p'}$. The operations $\mathsf{A}(z)$ are derived from a numerical solution of the Bloch-wave-coupled differential equations. Bloch waves happen to be a convenient representation for solving the Schrödinger equation, but it is equally possible to work with the plane-wave solutions of the Howie–Whelan equations. The wave vector at depth t_2 is related to the wave vector at depth t_1 by the matrix operator

$$\varphi(t_2) = \mathsf{P}(t_2 - t_1)\,\varphi(t_1). \quad (22a)$$

For a perfect crystal, the operator $\mathsf{P}(t_2 - t_1)$ can be expressed in terms of the Bloch-wave coefficients:

$$P_{gh}(t_2 - t_1) = \sum_j C_g^j\,C_h^j \exp[ik^j(t_2 - t_1)]. \quad (22b)$$

The beam amplitude at position $\mathbf{g} - \mathbf{q}$ in reciprocal space is given by

$$\frac{m}{\hbar^2 k}\int_0^T P'_{gh}(T-z)\,H_{h-l}\exp(-iq_z z)\,P_{l0}(z)\,\mathrm{d}z \quad (23)$$

and the intensity after summing over normal modes is

$$V\left(\frac{m}{2\pi\hbar^2 k}\right)^2 d\sigma \int_0^T P'_{gh}(T-z) \times P^{*\prime}_{gh'}(T-z)\,H_{h-l}\,H_{h'-l'}\,P_{l0}(z)\,P^*_{l'0}(z)\,\mathrm{d}z. \quad (24)$$

This approach was used by Gjønnes (1966) and can be easily related to the method given by Doyle (1969) who calculated the elastic scattering matrices by multislice methods.

It is possible to derive approximate solutions by assuming the dislocation is either in the top half or bottom half of the crystal. The appropriate term of the solution for the stacking-fault contrast is then applicable provided the stacking-fault operator is replaced by an appropriate operator for electron-beam propagation in a crystal with a dislocation.

The matrix elements for inelastic scattering

In the calculations, single inelastic scattering by phonons, plasmons and single-electron excitations has been considered.

The interaction between fast electrons and phonons has been described by a rigid ion model and the intensities arising from creating a phonon of wave vector $\mathbf{q}$ or destroying a phonon of wave vector $-\mathbf{q}$ have been summed. The matrix elements are the same as those used in Rez *et al.* (1977). For creation of a phonon of polarization p, wave vector $\mathbf{q}$, the matrix element is

$$H_g^{nm} = \frac{-i}{(MN)^{1/2}}(\mathbf{g}-\mathbf{q})\cdot\mathbf{e}_{q,p}\,V(\mathbf{g}-\mathbf{q}) \times \left(\frac{h}{2w_{\mathbf{q},p}}\right)^{1/2}(N_{\mathbf{q},p})^{1/2} \quad (25a)$$

and the matrix element for destruction of a phonon of wave vector $-\mathbf{q}$ is

$$H_g^{nm} = \frac{-i}{(MN)^{1/2}}(\mathbf{g}-\mathbf{q})\cdot\mathbf{e}_{\mathbf{q},p} \times V(\mathbf{g}-\mathbf{q})\left(\frac{h}{2w_{\mathbf{q},p}}\right)^{1/2}(N_{\mathbf{q},p}+1)^{1/2}, \quad (25b)$$

where $w_{\mathbf{q},p}$ is the phonon frequency, N is the number of atoms in the crystal, M is the atomic mass, $V(\mathbf{g}-\mathbf{q})$ a Fourier coefficient of the crystal potential and $N_{\mathbf{q},p}$, the occupation number of state $\mathbf{q}, p$, is given by

$$N_{\mathbf{q},p} = 1/[\exp(h w_{\mathbf{q},p}/k_B T) - 1], \quad (26)$$

where k_B is Boltzmann's constant and T the temperature. The phonon dispersion relation derived by Born (1942) for nearest-neighbor interactions in f.c.c. materials was used:

$$w^2 = \frac{3v_s^2}{a^2}(1 - \tfrac{1}{6}\{\cos[(q_x+q_y)a] + \cos[(q_y+q_z)a] + \cos[(q_z+q_x)a] - \cos[(q_x-q_y)a] - \cos[(q_y-q_z)a] - \cos[(q_z-q_x)a]\}), \quad (27)$$

where v_s is the appropriate sound velocity.

The plasmon matrix elements are those derived for a free electron gas as given by Ferrell (1956) for scattering between plane-wave fast-electron states and later used by Howie (1963) and Melander (1975). For plasmon scattering the Fourier coefficients of the interaction potential are

$$H_0^2 = \frac{e^2\,\Delta E}{2\varepsilon_0 q^2 V} \tag{28}$$

$H_g = 0$ in m.k.s. units, where q is the plasmon wave vector made up from the angular deflection q_x and the wave-vector difference due to the energy loss ΔE which is $k\Delta E/2E$.

$$q^2 = q_x^2 + k^2\,(\Delta E/2E)^2. \tag{29}$$

For single-electron scattering the product of the matrix elements $S^{i'p}\,S^{j'q}$ can be written as

$$S^{i'p}\,S^{j'q} = C_g^{i'}\,C_{g'}^{j'}\,H_{g-h}(q)\,H_{g'-h'}^{*}(q)\,C_h^p\,C_{h'}^q\,. \tag{30}$$

The products of the Fourier coefficients of the interaction potential have been derived by Kainuma (1955) using the completeness relation between final states, and the single-electron scattering is given by

$$\frac{1}{V_c V}\,C_g^{i'}\,C_{g'}^{j'}\left(\frac{e^2}{\varepsilon_0}\right)^2 \frac{S(g-h-q,\,q,\,+\,h'-g')}{|g-h-q|^2|q+h'-g'|^2}\,C_h^p\,C_{h'}^{q'}, \tag{31}$$

where

$$S(g-h-q,\,q+h'-g')$$

$$= \sum_k \exp\,[i(\mathbf{g}'-\mathbf{g}-\mathbf{h}'+\mathbf{h})\,\mathbf{r}_k]\left[\sum_n f_{nn}^k(g'-g-h'+h)\right.$$

$$\left. - \sum_{nm} f_{nm}^k(g-h-q)\,f_{nm}^k(h'-g'+q)\right]. \tag{32}$$

$f_{nm}^k(Q)$ is a matrix element and n, m refer to states of the kth atom in the unit cell.

This expression of course neglects the energy losses as it would then not be possible to use closure of final states, a severe disadvantage as these are difficult to calculate. This is important for small-angle scattering as has been pointed out by Pogany (1971). The matrix elements were calculated from values tabulated by Freeman (1959*a*,*b*) and the value needed for any particular argument was evaluated using a cubic spline interpolation. This procedure is probably appropriate for integrated low-loss scattering up to about 100 eV and gives a weighted average for the localization of scattering from the different subshells. As this is dominated by valence and conduction electrons, the results are not expected to be much different from those for plasmon excitations. If the contrast in a defect in a particular subshell is of interest, then the matrix element

$$\frac{1}{V_c V}\left(\frac{e^2}{\varepsilon_o}\right)^2 \frac{f(g-h-q)\,f^*(g'-h'-q)}{|g-h-q|^2\,|g'-h'-q|^2} \tag{33}$$

should be calculated from the appropriate oscillator strength as discussed by Leapman, Rez & Mayers (1980). This might show stronger localization effects particularly for deeply bound K shells.

Results

The contrast of a stacking fault ($\mathbf{g}.\mathbf{R} = -1/3$, $\mathbf{g} = 111$) in copper and a screw dislocation ($\mathbf{g}.\mathbf{b} = 1$, $\mathbf{g} = 111$) in aluminium is investigated for various apertures in a $11\bar{2}$ diffraction pattern when the crystal is set at the 111 diffraction position (Fig. 1). Aperture positions along the 111 systematic line and perpendicular to that line were considered. Only the results for point-aperture calculations are presented here as averaging over an aperture of given size did not usually have much effect. The intensities are therefore given as the differential cross section $\mathrm{d}I/\mathrm{d}\Omega$, and to obtain the intensity that would be observed with a given aperture the differential cross section should be multiplied by the aperture solid angle.

The results of plasmon scattering on the contrast of a stacking fault in a copper foil $4\xi_{111}$ thick are shown in Fig. 2. For apertures at the Bragg spots, the contrast is the same as in the elastically scattered electrons. As the

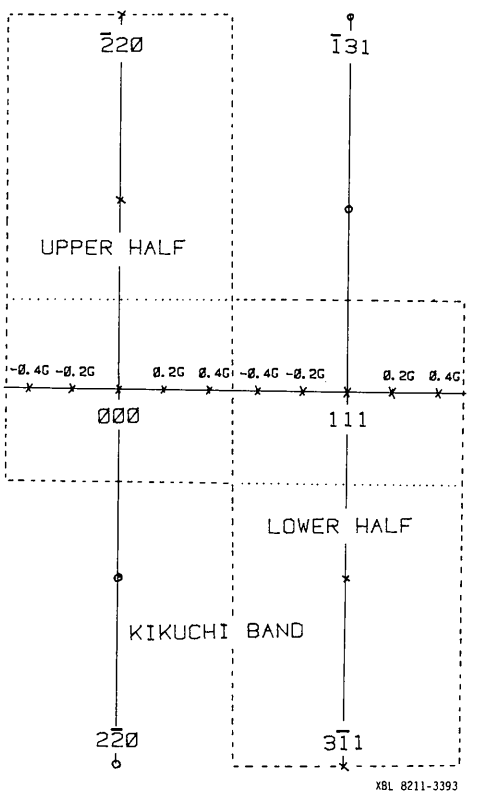

Fig. 1. $11\bar{2}$ diffraction pattern showing position of apertures used for the calculations.

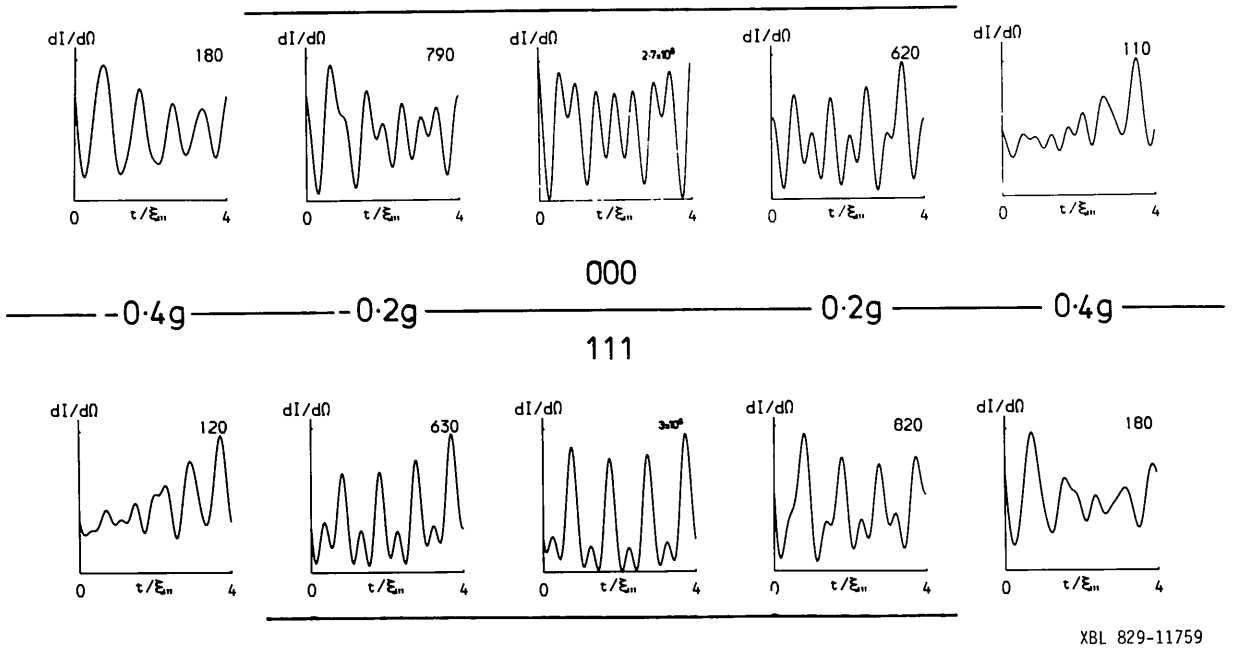

Fig. 2. Contrast in plasmon-scattered electrons for a stacking fault ($\mathbf{g}.\mathbf{R} = -1/3$, $\mathbf{g} = 111$) in a $4\xi_{111}$ thick copper foil for various aperture positions along a 111 systematic line.

scattering wave vector increases, the terms from contrast in both elastically and inelastically scattered electrons contribute to the contrast and these give rise to fringes of different periodicities. According to the theory, the contrast is also reduced as the Brillouin zone boundary is approached.

Any differences between single-electron contrast and plasmon contrast are due to differences in the Fourier coefficients of the interaction Hamiltonian. For single-electron excitations H_g/H_0 should be larger than for plasmons but the effect of this change is only noticed for the aperture position ($0{\cdot}4g$) close to the Brillouin zone boundary (Fig. 3). The effect should be more pronounced if localized excitations such as K shells were explicitly considered. There is also a change in contrast between plasmon and single-electron images for dislocations.

For phonon scattering, the first Fourier coefficient of the interaction potential H_g is either about equal to or greater than the mean coefficient H_0. This means that scattering is usually interbranch rather than intra-branch and it would not be expected that contrast would be preserved. For apertures on the Bragg spots there is no contrast, but as the aperture is displaced, either along the systematic line or perpendicular to it, the contrast increases (Figs. 4, 5). All inelastic images, whether phonon, plasmon or single electron, show the usual feature of elastic images in which fringes near the top are pseudo-complementary and fringes near the bottom are reversed for apertures placed near the incident beam and corresponding apertures placed near the diffracted beam.

Unlike the images in electrons scattered by plasmons or single-electron excitations, the stacking-fault images for phonon scattering perpendicular to the systematic line show reversed contrast to the elastic image. This

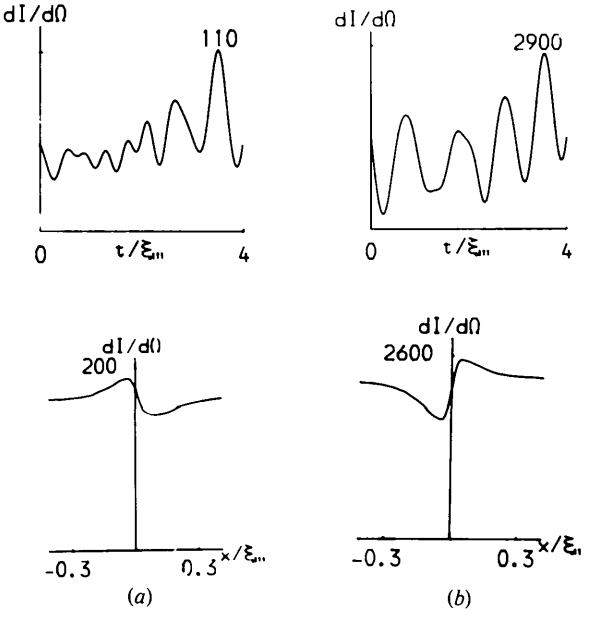

Fig. 3. Comparison of contrast for (*a*) plasmon excitation and (*b*) single-electron excitation for a stacking fault ($\mathbf{g}.\mathbf{r} = -1/3$, $\mathbf{g} = 111$) in copper (top row) and a dislocation ($\mathbf{g}.\mathbf{b} = 1$, $\mathbf{g} = 111$) in aluminium (bottom row).

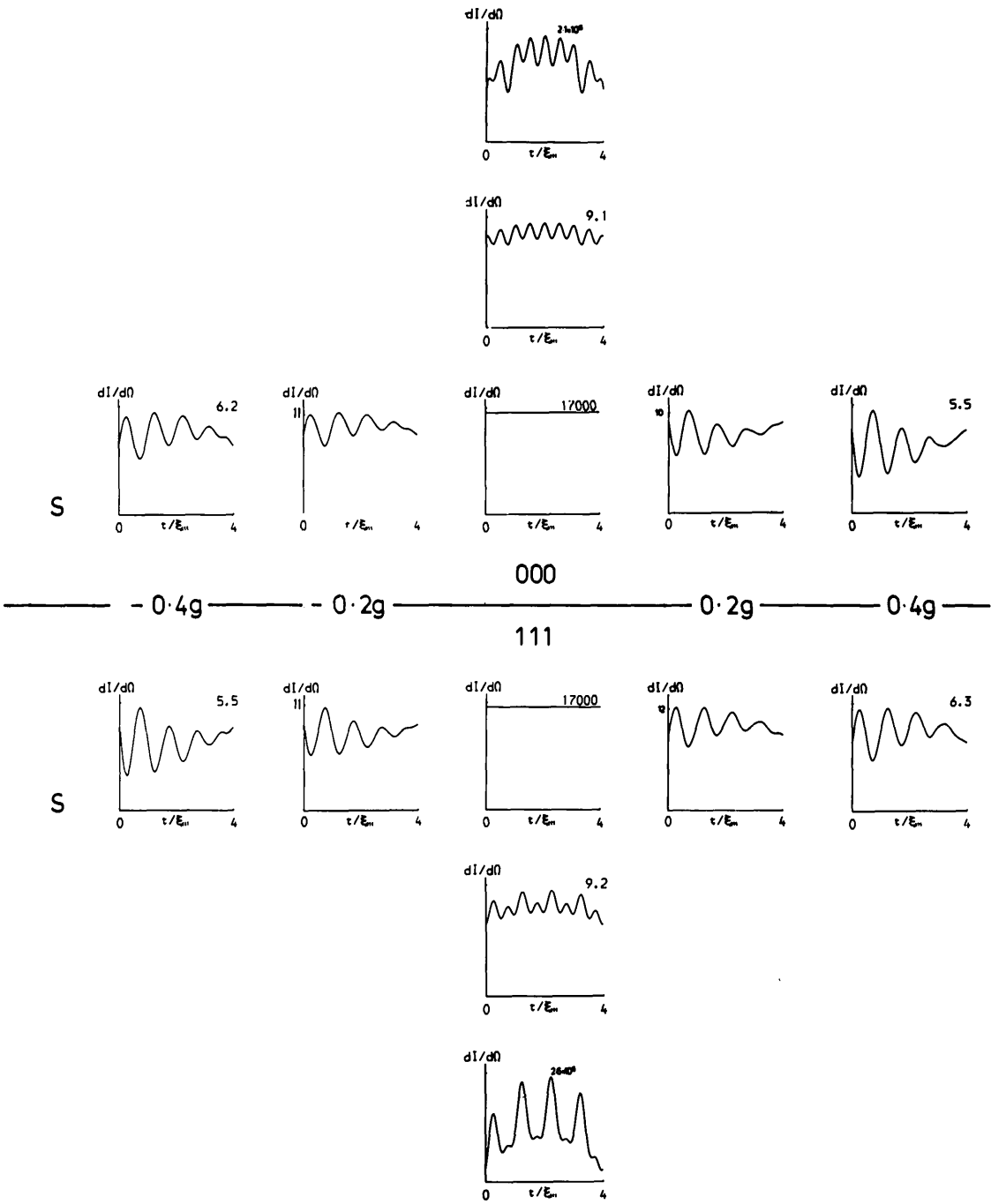

Fig. 4. Contrast of stacking fault ($\mathbf{g}.\mathbf{R} = -1/3$, $\mathbf{g} = 111$) for phonon-scattered electrons in a copper foil $4\xi_{111}$ thick for various aperture positions in a $11\bar{2}$ diffraction pattern.

can be explained by considering the matrix elements for large-angle scattering where $H_g \simeq H_0$ causing the matrix element S_{11} to dominate. This acts in opposition to anomalous absorption, so would increase those peaks which anomalous absorption decreased. Fig. 6 shows the result of a calculation with negative anomalous absorption of a stacking fault in elastically scattered electrons and this shows a similar reversal. A brief discussion of this effect is given by Kamiya & Nakai (1971).

Certain top–bottom effects are very apparent from the calculations. For apertures along the systematic line, the contrast is much stronger for a defect at the top of a foil and this has been observed, though for

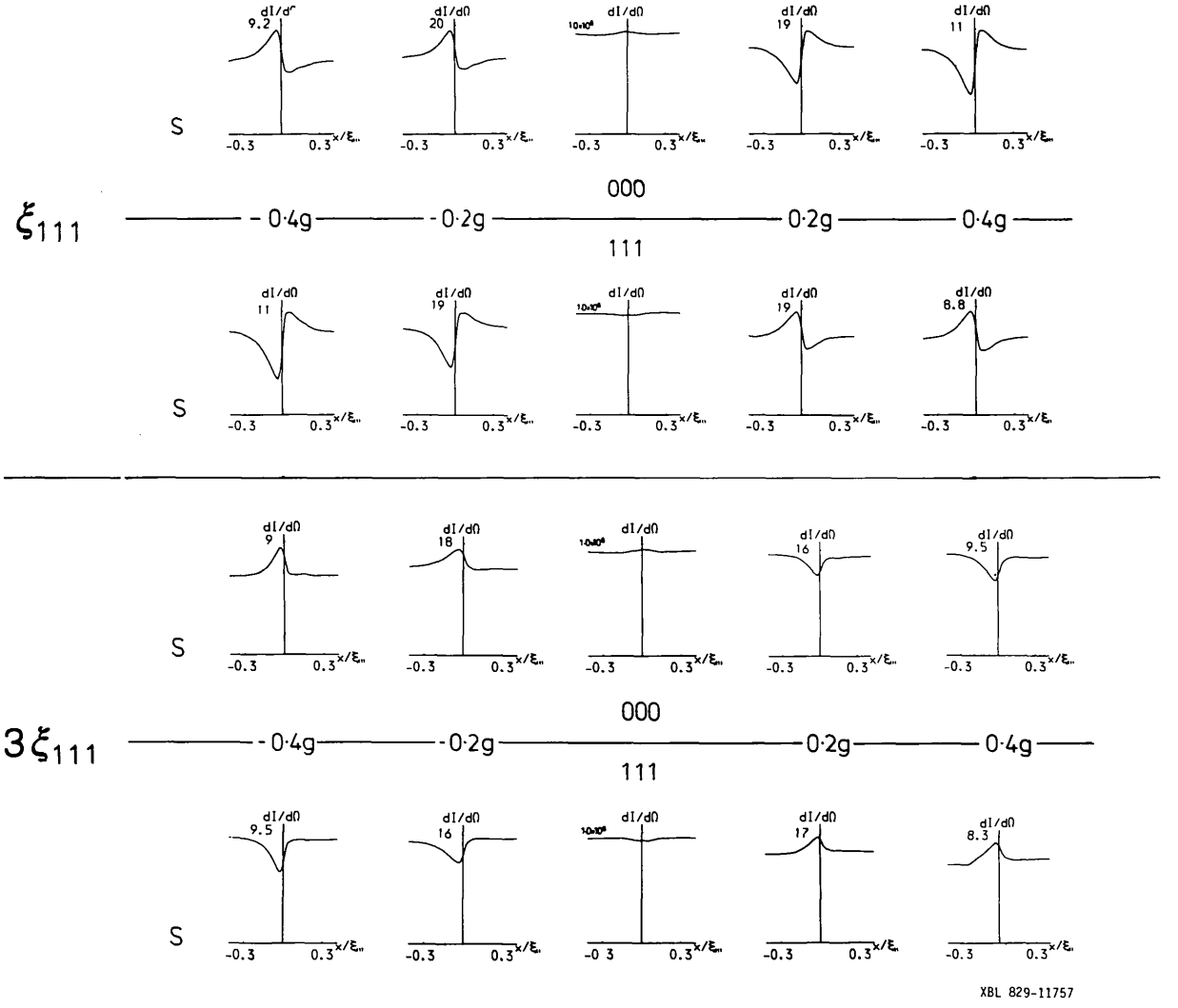

Fig. 5. Contrast of a screw dislocation ($\mathbf{g}.\mathbf{b} = 1$, $\mathbf{g} = 111$) in an aluminum foil $4\xi_{111}$ thick in phonon-scattered electrons for various aperture positions along a 111 systematic line. The profiles are given for a dislocation at a depth of ξ_{111} in the upper half and $3\xi_{111}$ in the lower half of the figure.

different aperture positions, by Kamiya & Nakai (1971). Furthermore, the contrast reverses from inside to outside the Kikuchi band and from an aperture near 000 (bright field) to a corresponding aperture near 111 (dark field).

For stacking faults, these effects can be understood from (15). The dominant contrast giving terms are those where (*a*) $i' = 1, j = 2, k'$ or $k = 1; j' = 1, i = 2, l$ or $l' = 2$, and (*b*) $i' = 2, j = 1, k'$ or $k = 1$; and $j' = 2$, $i = 1$, l or $l' = 2$. As can be seen, both involve interbranch transitions and both give rise to fringes of periodicity ξ_g. The contributions from these two terms cancel when the fault is near the bottom of the foil and so there is only contrast from faults closer to the top surface. Using the parameter β (Hirsch, Howie, Nicholson, Pashley & Whelan, 1965) to specify the inelastically scattered state the products of Bloch-wave coefficients are, for the first term of (15), $\frac{1}{2}\cos(\beta/2) \times \sin(\beta/2)$ for (*a*) and $-\frac{1}{2}\cos(\beta/2)\sin(\beta/2)$ for (*b*), so the two contributions cancel when inelastic scattering precedes stacking-fault scattering, which is dominant if the fault is at the bottom of the foil. For the second term of (15), the products of the Bloch-wave coefficients are $\frac{1}{2}\cos^2(\beta/2)$ and $-\frac{1}{2}\sin^2(\beta/2)$ for contributions (*a*) and (*b*) respectively. This means that for scattering by the stacking fault before inelastic scattering when the fault is at the top of the crystal there is contrast except for very small scattering angles when β is almost $\pi/2$. As the relative magnitudes of contributions (*a*) and (*b*) change as β goes through $\pi/2$, this also explains the reversal when going from one side of the Bragg spot to the other.

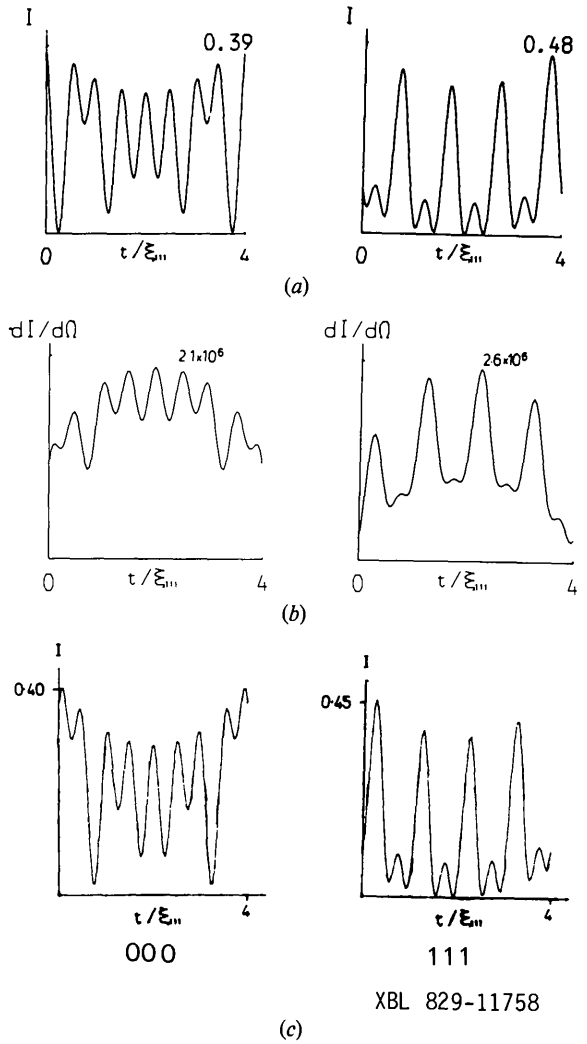

Fig. 6. Comparison of contrast of stacking fault in a copper foil $4\xi_{111}$ thick in (*a*) elastically scattered electrons, (*b*) electrons scattered to a position $2\bar{2}0$ by phonons, (*c*) elastically scattered electrons with negative anomalous absorption parameter.

Conclusions

As predicted by Howie (1963), Cundy *et al.* (1969) and Humphreys & Whelan (1969), the contrast of defects is similar to the contrast in elastically scattered electrons when the scattering is small-angle plasmon or single-electron scattering. For larger scattering angles, the contrast for plasmon and single-electron excitation can be partly understood by considering the dispersion surfaces for the incident and scattered states. Differences between the single-electron excitation contrast and plasmon contrast are only important for large scattering angles to positions near the Brillouin zone boundary.

For phonon scattering, there is no contrast for apertures centered on strongly excited Bragg spots, but the contrast gets stronger as the aperture is moved away from the Bragg spots, both along the systematic line and perpendicular to it. Defects at the top of a crystal show stronger contrast than defects at the bottom of a crystal.

For stacking faults, the contrast is reversed compared to the elastically scattered image when the aperture is displaced perpendicular to the systematic line in agreement with the experiments of Kamiya & Nakai (1971). This is because phonon scattering tends to act in the opposite sense to anomalous absorption.

I should like to thank Drs C. J. Humphreys and A. P. Young for useful discussions. Financial support was provided by the Science Research Council through a studentship and research fellowship while I was at the Department of Metallurgy and Science of Materials at the University of Oxford; and the NSF contract DMR 80-23461 while at Berkeley.

APPENDIX A

Equation (11) can be written as

$$\frac{d\psi(z)}{dz} = B(z)\,\psi(z),$$

$$\frac{d}{dz}G(z)\,\psi(z) = 0, \qquad (A1)$$

where G is a matrix

$$G(z)\frac{d\psi(z)}{dz} = -\frac{dG(z)}{dz}\psi(z)$$

$$\frac{d\psi(z)}{dz} = -G^{-1}(z)\frac{dG(z)}{dz}\psi(z) \qquad (A2)$$

$$B(z) = -G^{-1}(z)\frac{dG(z)}{dz}. \qquad (A3)$$

Integrating (*A*1) gives

$$G(t_1)\,\psi(t_1) = G(t_2)\,\psi(t_2) + \text{constant}. \qquad (A4)$$

The constant must be zero otherwise the solution would be inconsistent at $t_1 = t_2$, so

$$\psi(t_1) = G^{-1}(t_1)\,G(t_2)\,\psi(t_2), \qquad (A5)$$

and comparing this with (12) gives

$$A(t_1 - t_2) = G^{-1}(t_1)\,G(t_2). \qquad (A6)$$

Taking the inverse of both sides,

$$A^{-1}(t_1 - t_2) = G^{-1}(t_2)\,G(t_1) = A(t_2 - t_1), \qquad (A7)$$

which means that the matrix relating the solution at depth t_1 to that at depth t_2 is the inverse of the matrix

relating the solution at t_2 to that at t_1. These properties of the equations are the basis of the generalized cross section of Head, Humble, Clarebrough, Moreton & Forwood (1973) which considerably speeds up the calculation of dislocation images.

APPENDIX B

The equations relating the amplitudes are

$$\frac{d\psi'(z)}{dz} = B'(z)\,\psi'(z) + S(z)\exp(-iq_z z)\psi(z) \quad (B1)$$

$$\frac{d\psi(z)}{dz} = B(z)\,\psi(z), \quad (B2)$$

where the elements of $B(z)$ are

$$\sum_g C_g^i C_g^j \frac{\mathbf{g}.\mathbf{du(r)}}{dz} \exp[i(k^j - k^i)\,z]$$

and scattered states are denoted by primed quantities:

$$\frac{d[G'(z)\,\psi'(z)]}{dz} = G'(z)\,S(z)\exp(-iq_z z)\,\psi(z) \quad (B3)$$

$$[G'(z)\,\psi'(z)]_0^T = \int_0^T G'(z)\,S(z)\exp(-iq_z z)\,\psi(z)\,dz \quad (B4)$$

$$\psi'(T) = G'^{-1}(T)\,G'(0)\,\psi'(0) + G'^{-1}(T) \times \int_0^T G'(z)S(z)\exp(-iq_z z)\,\psi(z)\,dz. \quad (B5)$$

As no inelastic scattering takes place before the fast electron enters the crystal $\psi'(0) = 0$ and, using (A6),

$$\psi'(T) = \int_0^T A'(T-z)\,S(z)\exp(-iq_z z)\,\psi(z)\,dz, \quad (B6)$$

which is the same as (13).

References

BORN, M. (1942). *Rep. Prog. Phys.* **9**, 296–333.
CASTAING, R., EL HILI, A. & HENRY, L. (1966). *C.R. Acad. Sci.* **262**, 169–172.
CRAVEN, A. J., GIBSON, J. M., HOWIE, A. & SPALDING, D. R. (1978). *Philos. Mag.* **38**, 519–527.
CUNDY, S. L., HOWIE, A. & VALDRE, U. (1969). *Philos. Mag.* **20**, 147–163.
DOYLE, P. A. (1969). *Acta Cryst.* A**25**, 569–577.
EL HILI, A. (1967). *J. Microsc. (Paris)*, **6**, 693–724.
FERRELL, R. A. (1956). *Phys. Rev.* **101**, 554–563.
FREEMAN, A. J. (1959*a*). *Phys. Rev.* **113**, 176–178.
FREEMAN, A. J. (1959*b*). *Acta Cryst.* **12**, 274–279.
GAI, P. L. & HOWIE, A. (1975). *Philos. Mag.* **31**, 519–528.
GJØNNES, J. (1966). *Acta Cryst.* **20**, 240–249.
HEAD, A. K., HUMBLE, P., CLAREBROUGH, L. M., MORETON, A. J. & FORWOOD, C. T. (1973). *Defects in Crystalline Solids*, 7. Amsterdam: North Holland.
HIRSCH, P. B., HOWIE, A., NICHOLSON, R. B., PASHLEY, D. W. & WHELAN, M. J. (1965). *Electron Microscopy of Thin Crystals*. London: Butterworths.
HOWIE, A. (1963). *Proc. R. Soc. London Ser. A*, **271**, 268–287.
HUMPHREYS, C. J. & WHELAN, M. J. (1969). *Philos. Mag.* **20**, 165–172.
KAINUMA, Y. (1955). *Acta Cryst.* **8**, 247–257.
KAMIYA, Y. & NAKAI, Y. (1971). *J. Phys. Jpn*, **31**, 195–203.
KAMIYA, Y. & NAKAI, Y. (1976). *J. Phys. Soc. Jpn*, **40**, 1690–1697.
KAMIYA, Y. & UYEDA, Y. (1961). *J. Phys. Soc. Jpn*, **16**, 1361–1366.
LEAPMAN, R. D., REZ, P. & MAYERS, D. F. (1980). *J. Chem. Phys.* **72**, 1232–1243.
MELANDER, A. (1975). *Philos. Mag.* **31**, 599–608.
MELANDER, A. & SANDSTROM, R. (1975*a*). *Acta Cryst.* A**31**, 116–125.
MELANDER, A. & SANDSTROM, R. (1975*b*). *J. Phys. C*, **8**, 767–779.
NONOYAMA, M., NAKAI, Y. & KAMIYA, Y. (1973). *J. Electron Microsc.* **22**, 231–241.
POGANY, A. P. (1971). Proc. 25th Anniv. Meeting EMAG, Cambridge, pp. 64–65.
REZ, P., HUMPHREYS, C. J. & WHELAN, M. J. (1977). *Philos. Mag.* **35**, 81–96.
YOSHIOKA, H. (1957). *J. Phys. Soc. Jpn*, **12**, 618–628.
YOUNG, A. P. & REZ, P. (1975). *J. Phys. C*, **8**, L1–L7.

Acta Cryst. (1983). A**39**, 706–711

Contrast Variation of the Small-Angle Neutron Scattering of Globular Particles: the Influence of Hydrogen Exchange

BY J. WITZ

Département de Virologie, Institut de Biologie Moléculaire et Cellulaire du CNRS, 15, rue Descartes, 67000 Strasbourg, France

(*Received* 4 *January* 1983; *accepted* 7 *April* 1983)

Abstract

The influence of hydrogen/deuterium exchange on the intensity scattered by solutions of globular particles in neutron small-angle scattering experiments in ^2H_2O/^1H_2O buffers has been calculated. By separating the contribution of the change of the average scattering density of the solute from that of the inhomogeneities of the distribution of exchangeable hydrogens, equations similar to the classical equations of Stuhrman & Kirste

0108-7673/83/050706-06$01.50